ELSEVIER

Journal of Organometallic Chemistry 627 (2001) 189–200

Journal of Organometallic Chemistry

www.elsevier.nl/locate/jorganchem

Further studies on dialkyltin 1,3-dithiole-2-thione-4,5-dithiolates, $R_2Sn(dmit)$. Crystal structures of orthorhombic- and monoclinic-$Et_2Sn(dmit)$, and $Me_2Sn(dmit)$

Gillian M. Allan [a], R. Alan Howie [a,*], Janet M.S. Skakle [a], James L. Wardell [a,b], Solange M.S.V. Wardell [c]

[a] *Department of Chemistry, University of Aberdeen, Meston Walk, Old Aberdeen AB24 3UE, Scotland, UK*
[b] *Departamento de Química Inorgânica, Instituto de Química, Universidade Federal do Rio de Janeiro, 21945-970 Rio de Janeiro, RJ, Brazil*
[c] *Instituto de Química, Departamento de Química Orgânica, Universidade Federal Fluminense, 24020-150 Niterói, RJ, Brazil*

Received 8 January 2001; received in revised form 15 February 2001

Abstract

The crystal structures of orthorhombic and monoclinic diethyltin bis(1,3-dithiole-2-thione-4,5-dithiolate), [$Et_2Sn(dmit)$], *ortho*-**3** and *mono*-**3**, and dimethyltin bis(1,3-dithiole-2-thione-4,5-dithiolate) (**4**) have been determined. Transformation of solid *ortho*-**3** to *mono*-**3** occurs at 139–140°C. Molecules of *ortho*-**3**, obtained by recrystallisation from aqueous acetone, and **4**, are linked into chains as a result of intermolecular Sn–thione S(5) interactions: the tin centres are penta-coordinate with distorted trigonal bipyramidal geometries. The intermolecular, Sn–S(5) thione bonds {3.0083(15) Å in *ortho*-**3** at 150 K [3.037(4) at 298 K], and 3.001(2) and 2.960(2) Å in the two independent molecules of **4** at 150 K}, are considerably longer than the primary intramolecular Sn bonds to the dithiolato S atoms [between 2.440(3) and 2.5235(15) Å]. The two independent molecules of *mono*-**3**, obtained from aqueous methanol, have quite different arrangements: tin atoms in molecule A form two relatively weak intermolecular Sn–thione S bonds, 3.567(2) and 3.620(3) Å, with the formation of sheets, while those in molecule B form one similar bond, Sn–S = 3.555(2) Å to give chains, with a much longer contact, Sn···S = 3.927(2) Å to another chain. The latter is only ca. 0.12 Å less than the van der Waals radii sum for Sn and S. Sulfur–sulfur contacts, within the sum of the van der Waals radii of two S atoms, 3.60 Å, in **3** and **4**, not only reinforce the chains but also help to establish 3D networks.

Keywords: Organotin; 1,3-Dithiole-2-thione-4,5-dithiolate; Crystal structures; Polymorphism

1. Introduction

Diorganotin derivatives of 4,5-dimercapto-1,3-dithiole-2-thione, H_2-dmit, **1**, have been previously studied [1–3]: both ionic species, [Q][$R_2SnX(dmit)$], **II** [1], and neutral compounds, $R_2Sn(dmit)$, **I**, [2,3] have been obtained (Q = onium cation; R = Me, Ph, etc.; X = halide or pseudohalide). The compounds, [Q][R_2SnX-(dmit)], (**II**: e.g. Q = NBu_4, R = Me, X = Cl; Q = 1,4-dimethylpyridinium, R = Ph, X = NCS, Br or I/Cl), have similar structures, with non-interacting cation and anions, and with distorted trigonal bipyramidal, five-

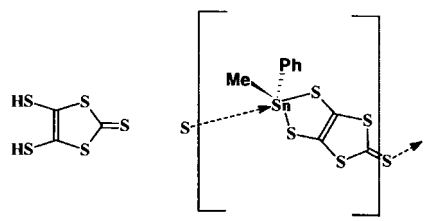

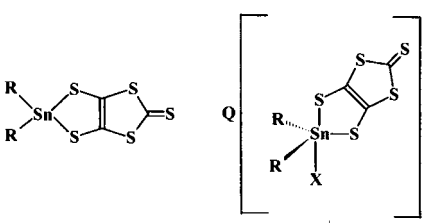

* Corresponding author. Tel.: +44-1224-272907; fax: +44-1224-272921.
E-mail address: r.a.howie@abdn.ac.uk (R.A. Howie).

0022-328X/01/$ - see front matter
PII: S0022-328X(01)00735-5

coordinate, tin centres [1]. As shown by NMR spectral data, **II** remain penta-coordinate species in non-aqueous solution, but in aqueous media, however, they dissociate to yield **I** and [Q]X [1,2].

The tin centre in solid PhMeSn(dmit), **2**, is five-coordinate with a trigonal bipyramidal geometry: molecules are linked into spiral chains via intermolecular Sn–S(thione) interactions [2]. The X-ray structure determination of **2** revealed only one type of tin centre, which was confirmed by the single δ^{119}Sn value (94.9 ppm) in the solid state ^{119}Sn-NMR spectrum. In contrast, solid state ^{13}C- and ^{119}Sn-NMR spectra of an analytically pure sample of $Et_2Sn(dmit)$, **3**, obtained by relatively fast crystallisation from aqueous acetone, indicated that the sample contained tin in different sites [2]. The solid state δ^{119}Sn spectrum for this sample of **3** had a peak at 153.7 and an envelope of values between 110 and 128, with maxima at 121.3 and 127.5 ppm, compared to the single solution (Me_2CO) value of 165.7 ppm.

A further study has now been carried out in order to establish whether these solid state NMR chemical shift values arose from a single crystalline phase or from mixed polymorphic phases. We now report our results for **3** and further information on other known alkyl derivatives of **I**, namely $Me_2Sn(dmit)$ (**4**) and $Bu_2Sn(dmit)$ (**5**), as well as the new compound, (n-$C_{14}H_{29})_2Sn(dmit)$ (**6**).

2. Results and discussion

2.1. General

The dialkyltin dithiolates, **3**–**6**, were obtained from the reaction of diorganotin dihalides with $[NEt_4]_2[Zn(dmit)_2]$ in acetone solution, using a modification of a previously reported procedure [2]. The initial products were isolated on addition of water to the acetone solution, with subsequent recrystallisations from a particular organic medium. The spectra of each compound, determined in acetone solution, were found to be the same no matter what solvent was used in the crystallisation. The δ^{119}Sn values are indicative of higher-coordinate tin species in solution. The lower alkyl compounds, **3** and **4**, are stable on storage in air at ambient temperature: as the organic chain increased in length the ease of handling decreased. Compound **6**, in particular, darkened appreciably on storage in air. However, TGA studies indicated that the onset of thermal decomposition of **6**, under nitrogen, was at a higher temperature than found for either **3** or **5**, see Table 1. TGA, linked with mass spectroscopy, showed common m/e fragments for **3**–**6**, indicating that fragmentation occurred to a significant extent within the dithiolate ligand.

2.2. Solid state study of *3*

The solid state ^{119}Sn-NMR spectra of the sample of **3**, isolated in this study on addition of water to the reaction mixture containing Et_2SnBr_2 and $[NEt_4]_2[Zn(dmit)_2]$ in acetone, was somewhat different from that reported for the sample of **3** used in our earlier study [2]. The present sample had δ^{119}Sn values at 158.2, 112.1 and 123.4 ppm, see Fig. 1, while the earlier sample had a single peak at 153.7 with an envelope of peaks between 110 and 128, with spikes at 121.3 and 127.5 ppm [2]. Side band analysis of the current sample indicated that two (123.4 and 158.2 ppm) of the three signals arose from similar site geometries. As subsequent study showed that different crystal forms can indeed be obtained, these differences are accounted for by the use of different crystallisation media resulting in the production of phases in different proportions. Two different crystalline phases of **3** have now been confirmed: slow recrystallisation of **3** from acetone produced an orthorhombic form, *ortho*-**3**, while recrystallisation from aqueous MeOH gave a monoclinic form, *mono*-**3**, structural details are discussed below. Crystallisations, from other solvent systems, such as CH_2Cl_2–petroleum ether (mixture of both forms obtained) and $CHCl_3$, were also investigated but no clear-cut evidence for other phases was found, using X-ray powder diffraction patterns. The sample obtained by recrystallisation from $CHCl_3$ solution did show differences with the other confirmed two phases, but crystals suitable for X-ray study could not be produced. The differences, largely in

Table 1
Decomposition temperature and weight loss, obtained by TGA–MS, and m.p. [a]

Compound	Decomposition onset	Weight loss% at °C				Mass fragments (m/e)	Melting point
		200	250	300	350		
4	203	0	10	19	25	44, 64, 76, 94	222–226
3	120	5	12	21	26	44, 64, 76, 126	205–208
5	148	2	14	41	43	44, 64, 76, 86	197–200
6	158	0.4	0.9	3	28	44, 54, 64, 68, 76	170–174

[a] As measured on a Kofler hotstage.

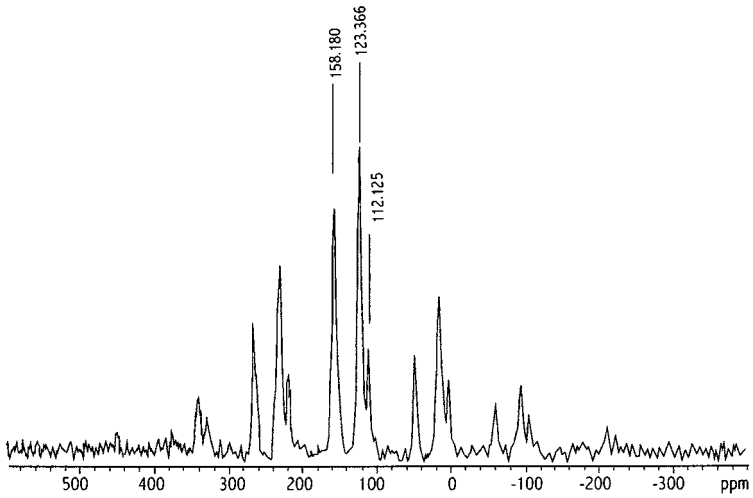

Fig. 1. Solid state ^{119}Sn-NMR spectrum of a sample of **3**, obtained by crystallisation from aqueous acetone solution.

relative intensities, could have arisen from preferred orientation rather than from a different crystalline phase.

DSC studies, combined with X-ray powder diffraction, indicated the orthorhombic to monoclinic phase change occurred on heating solid *ortho*-**3** at ca. 139–140°C, the melting point of all samples of **3** being between 205 and 208°C. Fig. 2 shows the powder patterns obtained for the change of *ortho*-**3** to *mono*-**3**, as well as the theoretical patterns calculated from the X-ray single crystal data. Further heating beyond the melting point led to unresolvable powder patterns, mainly due to partial decomposition of the sample.

2.3. Crystal structures of ortho-*3* and mono-*3*

The general atom numbering system used for molecules of both *ortho*-**3** and *mono*-**3** is shown in Fig. 3. In all cases, primary bonds to tin are formed by the two ethyl groups and the chelating dmit dithiolato S atoms, S(1) and S(2): additional and weaker secondary bonds to tin, involving thione S atoms, S(5) of adjacent molecules, vary with the particular molecule. The four primary bond lengths [Sn–C between 2.108(11) and 2.153(5) Å, and Sn–S between 2.435(4) and 2.5235(15) Å] are in the expected regions.

2.3.1. ortho-*3*

Data were collected at two temperatures, 150(2) and 298(2) K for *ortho*-**3**. No structural change occurred between the two temperatures, but there is, as expected, a reduction in the unit cell volume (ca. 1.5%) on reducing the temperature. Selected bond lengths and angles are displayed in Table 2 for the determinations at both temperatures: the data discussed in this section are those obtained at 150(2) K, unless otherwise indicated. The structure is in a non-centrosymmetric space group, $Pna2_1$. However, it is racemic, due to the glide planes, but it is polar, i.e. all the molecules are aligned in the same direction.

Molecules of *ortho*-**3** are linked to form infinite chains, parallel to *c*, by intermolecular tin–thione sulfur, $(S5)^{i}$, bonds of length 3.0083(15) Å at 150 K [3.037(4) Å) at 298 K], see Fig. 4a (symmetry operation (i): $x, y, z+1$). While these Sn–S distances are much longer than a single Sn–S bond length, they are well within the sum of the van der Waals radii, 4.05 Å [5,6]. The geometry at tin, thereby, becomes distorted trigo-

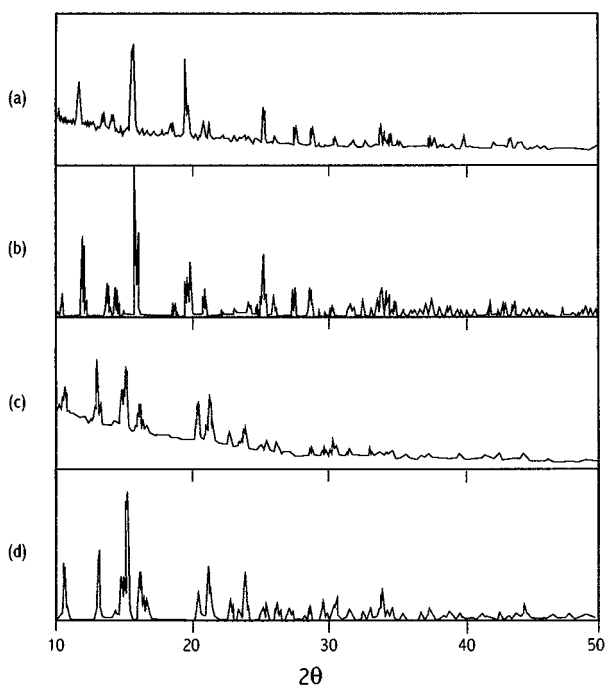

Fig. 2. X-ray powder diffraction patterns for **3**: (a) *ortho*-**3**; (b) theoretical pattern for *ortho*-**3**, calculated from single crystal structure data; (c) product of heating *ortho*-**3** at 140°C; (d) theoretical pattern for *mono*-**3**, calculated from single crystal structure data.

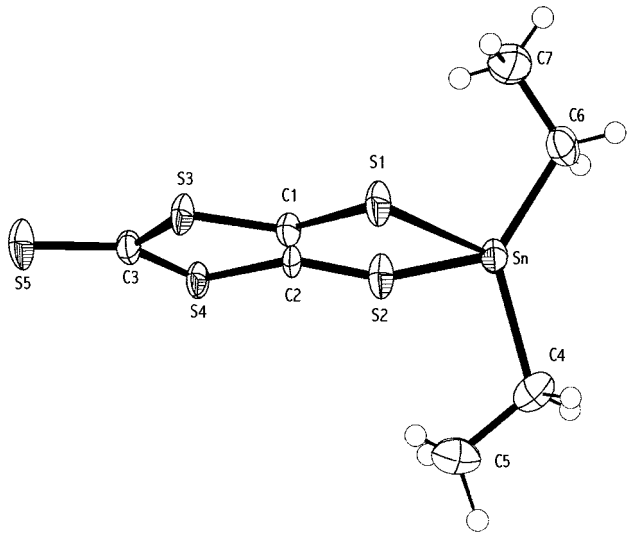

Fig. 3. The general atom numbering system used for molecules of *ortho*-**3** and *mono*-**3**. The particular molecule presented is *ortho*-**3** at 150 K. Probability ellipsoids are drawn at 50%.

Table 2
Selected bond lengths (Å) and angles (°) in *ortho*-**3**[a]

	298(2) K	150(2) K
Sn–C(6)	2.137(15)	2.153(5)
Sn–C(4)	2.115(13)	2.145(6)
Sn–S(2)	2.513(4)	2.5235(15)
Sn–S(1)	2.436(4)	2.4590(14)
Sn–S(5)^{i}	3.037(4)	3.0083(15)
S(1)–C(1)	1.748(11)	1.740(5)
S(2)–C(2)	1.741(12)	1.754(6)
S(3)–C(3)	1.724(13)	1.713(5)
S(3)–C(1)	1.718(11)	1.742(5)
S(4)–C(3)	1.712(14)	1.721(5)
S(4)–C(2)	1.749(14)	1.740(7)
S(5)–C(3)	1.639(12)	1.668(5)
C(1)–C(2)	1.349(16)	1.357(8)
C(4)–Sn–C(6)	128.7(8)	130.8(2)
C(6)–Sn–S(2)	101.4(5)	101.56(15)
C(4)–Sn–S(2)	100.6(4)	100.96(19)
C(6)–Sn–S(1)	113.0(6)	111.07(16)
C(4)–Sn–S(1)	113.1(5)	112.77(17)
S(1)–Sn–S(2)	88.90(12)	88.32(4)
C(6)–Sn–S(5)^{i}	88.9(5)	89.12(15)
C(4)–Sn–S(5)^{i}	86.0(4)	85.60(18)
S(2)–Sn–S(5)^{i}	159.53(10)	158.26(4)
S(1)–Sn–S(5)^{i}	70.74(10)	70.11(4)
C(2)–S(2)–Sn	96.6(4)	97.2(2)
C(1)–S(1)–Sn	99.4(4)	98.92(18)
C(3)–S(5)–Sn^{ii}	112.1(5)	111.1(2)

[a] Symmetry operation: (i) $x, y, z+1$; (ii) $x, y, z-1$.

nal bipyramidal with the S(5)^{i} atom and a dithiolato S atom, S(2), in axial sites, with S(2)–Sn–S(5)^{i} = 158.26(4)°. This departure from the ideal angle of 180° is not imposed by the chelate bite angle, as this is close to the ideal of 90° [S(1)–Sn–S(2) = 88.32(4)°], but rather by the weakness of the intermolecular interaction, which results in the geometry at the tin centre retaining some tetrahedral character. The distance in which the tin is out of the equatorial plane [0.297(3) Å at 150 K and 0.289(9) Å at 298 K] is a further indicator of this. As expected, the axial tin–dithiolate bond, Sn–S(2) = 2.5235(15) Å, is longer than the equatorial bond, Sn–S(1) = 2.459(14) Å.

The C=C and the attached S atoms in the dmit ligand are essentially co-planar; consequently, these atoms are used as the dmit reference plane. The Sn and thione S atoms are out of this plane by 0.304(2) and −0.127(3), respectively, at 150 K, and 0.144(6) and −0.100(8), respectively, at 298 K [the opposite signs indicate the Sn(dmit) fragments have overall chair conformations].

In addition to the Sn–S(5)^{i} intermolecular interactions, there are S(5)···S(1)^{i} contacts at 3.1721(18) Å, which reinforce the primary chains, Fig. 4b. The van der Waals radius for S is quoted as 1.80 Å in Ref. [5] and as 1.85 Å in Ref. [6]: the value taken in this paper is the lower of these two values. Other S···S contacts, [S(1)···S(3)^{ii} = 3.5372(19) Å, seen in pairs around the mid-points of the cell edges, S(1)···S(2)^{iii} = 3.509(2) and S(2)···S(3)^{iv} = 3.4695(19) Å: symmetry operations — (ii) $-x-1, -y, z+1/2$; (iii) $x-1/2, -y-1/2, z$; (iv) $x+1/2, -y-1/2, z$] link the primary chains into a 3D network, in such a way that the ethyl groups are found in channels, parallel to *c*, bounded by six primary chains, see Fig. 4b. However, at 298 K, these S···S interchain separations increase to > 3.6 Å.

2.3.2. *mono*-**3**

Data for *mono*-**3** were collected at 298(2) K. Selected bond lengths and angles for *mono*-**3** are displayed in Table 3. There are two independent molecules, A and B, in the asymmetric unit cell, each having similar molecular arrangements, but having different intermolecular interactions, see Fig. 5a and b. Molecule A forms two similar-strength intermolecular Sn–S(thione) interactions [Sn(1A)–S(5A)^{i} = 3.567(2) and Sn(1A)–S(5A)^{ii} = 3.620(3) Å], which link the molecules into layers or sheets; each thione S atom acts as a bridge between three molecules. In contrast in molecule B, there is only one Sn–thione S intermolecular interaction [Sn(1B)–S(5B)^{i} = 3.555(2) Å], comparable to that in molecule A, which provides chains in the direction of *a*: in addition, there is a very much longer intermolecular tin–thione separation, [Sn(1B)–S(5B)^{iii} = 3.927(2) Å], between adjacent chains [symmetry operations — (i) $x+1, y, z$; (ii) $x+1/2, -y, z-1/2$; (iii) $x+1/2, -y+1, z-1/2$]. The latter distance is only ca. 0.12 Å less than the van der Waals radii sum, 4.05 Å, for Sn and S [4,5] and thus constitutes at best a very weak interaction. It is noticeable how much weaker are the individual Sn–S interactions in both molecules of *mono*-**3** compared to those in *ortho*-**3**. Taking into account both the secondary Sn–thione S intermolecular interac-

tions with the four stronger primary bonds, the tin centre in molecule A is six-coordinate with a geometry far removed from any regular array. The geometric situation in molecule B could also be considered to be somewhat related if the long Sn(1B)–S(5B)^{iii} separation is included as an interaction. The Sn and thione S atoms are out of the best dmit plane, by 0.141(4) and 0.053(5) Å, respectively, in molecule B, i.e. the [Sn-(dmit)] fragment has an overall boat shape: in molecule A, only the Sn atom is out of the dmit plane by 0.177(4) Å, so an envelope conformation is present. Fig. 5c illustrates the content of the unit cell viewed down *a*. The molecules form layers perpendicular to *b* with only molecules A in the layer with $y = 0$ (and $y = 1$) and only molecules of B in the layer with $y = 1/2$. Within each layer, the molecules are related to one another by cell translations and the operation of a crystallographic *n*-glide. The ethyl groups appear on each side of the layers. Chains of molecules of A and of B are each reinforced by appropriate S(5)···S(2)^{i} contacts: S(2A)···S(5A)^{i} = 3.396(3) and S(2B)···S(5B)^{i} = 3.374(3) Å. The links between chains of molecules A, to form layers or sheets, involve S(1A)···S(5A)^{ii} and S(1A)···S(2A)^{iii} contacts at 3.272(3) and 3.511(4) Å, respectively. Links between chains of molecules of B involve S(1B)···S(5B)^{ii} contacts at 3.503(4) Å; symmetry operations: (i) $x + 1, y, z$; (ii) $x + 1/2, -y, z - 1/2$; (iii) $x - 1/2, -y, z - 1/2$. The structural differences between molecules A and B result from their orientations with respect to the crystallographic *n*-glide with which each is associated. Tin bonding to the dmit chelates is more symmetrical in *mono*-**3** than in *ortho*-**3**: Sn(1A)–S(1A) = 2.460(3) and Sn(1A)–S(2A) = 2.449(3) Å, Sn(1B)–S(1B) = 2.458(3) and Sn(1B)–S(2B) = 2.447(3) Å, in *mono*-**3** compared to the values 2.436(4) and 2.513(4) Å in *ortho*-**3** at 298(2) K.

2.4. Solid state study of **4**

Analytically pure samples of **4**, recrystallised from the reaction mixture in acetone on addition of water, and from a subsequent recrystallisation from aqueous methanol had very similar DSC traces and X-ray powder patterns. Very small endothermic peaks were present in the DSC trace of both samples, prior to fusion at ca. 226–228°C and 222–225°C, for the aqueous acetone and aqueous methanol recrystallised materials, respectively. Further heating to 400°C resulted in two further small exothermic peaks in each case. No peaks were, however, observed in the DSC traces on subsequent cool/reheat cycles to 400°C. TGA indicated that weight loss began at ca. 210°C, i.e. just

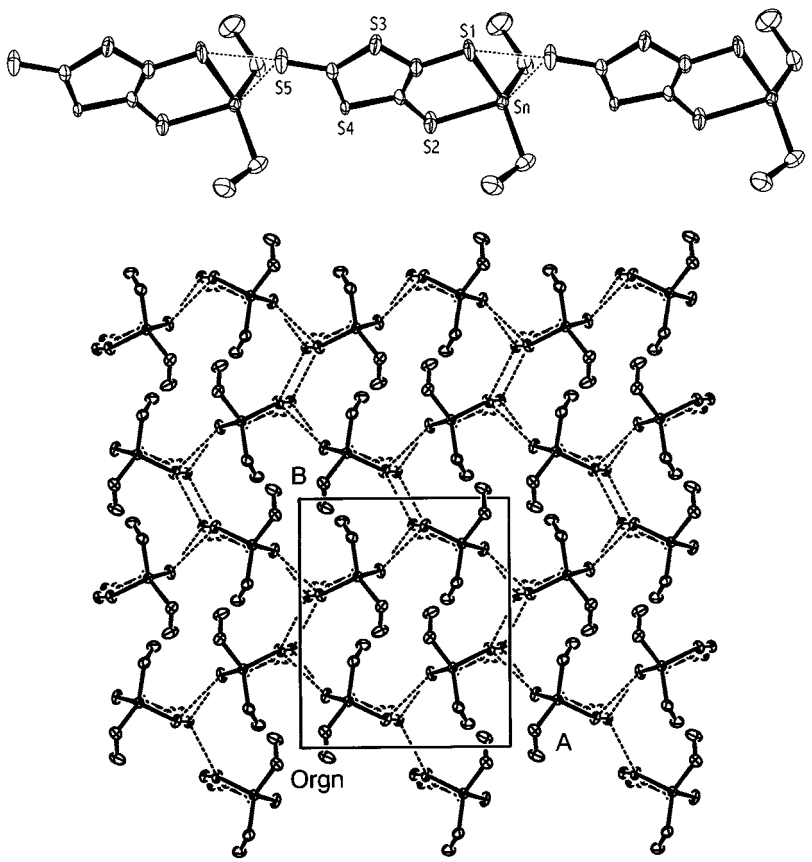

Fig. 4. (a) Part of a chain of molecules of *ortho*-**3**, parallel to *c*. (b) The 3D network of *ortho*-**3** at 150 K, resulting from intermolecular S···S contacts. Probability ellipsoids are drawn at the 50% level.

Table 3
Selected bond lengths (Å) and angles (°) in *mono*-**3** at 298 K[a]

Sn(1A)–C(6A)	2.116(9)	Sn(1B)–C(6B)	2.108(11)
Sn(1A)–C(4A)	2.123(9)	Sn(1B)–C(4B)	2.115(9)
Sn(1A)–S(2A)	2.449(2)	Sn(1B)–S(2B)	2.447(3)
Sn(1A)–S(1A)	2.460(2)	Sn(1B)–S(1B)	2.458(3)
Sn(1A)–S(5A)^{i}	3.567(2)	Sn(1B)–S(5B)^{i}	3.555(2)
Sn(1A)–S(5A)^{ii}	3.620(3)	Sn(1B)–S(5B)^{iii}	3.927(2)
S(1A)–C(1A)	1.750(7)	S(1B)–C(1B)	1.747(8)
S(2A)–C(2A)	1.740(6)	S(2B)–C(2B)	1.729(7)
S(3A)–C(3A)	1.708(8)	S(3B)–C(3B)	1.699(8)
S(3A)–C(1A)	1.723(7)	S(3B)–C(1B)	1.734(7)
S(4A)–C(3A)	1.714(7)	S(4B)–C(3B)	1.713(7)
S(4A)–C(2A)	1.747(6)	S(4B)–C(2B)	1.735(7)
S(5A)–C(3A)	1.662(7)	S(5B)–C(3B)	1.669(7)
C(1A)–C(2A)	1.335(10)	C(1B)–C(2B)	1.357(11)
C(4A)–Sn(1A)–C(6A)	126.3(3)	C(4B)–Sn(1B)–C(6B)	119.5(5)
C(6A)–Sn(1A)–S(2A)	111.5(3)	C(6B)–Sn(1B)–S(2B)	112.1(5)
C(4A)–Sn(1A)–S(2A)	106.3(3)	C(4B)–Sn(1B)–S(2B)	110.7(3)
C(6A)–Sn(1A)–S(1A)	107.2(3)	C(6B)–Sn(1B)–S(1B)	110.1(3)
C(4A)–Sn(1A)–S(1A)	110.1(3)	C(4B)–Sn(1B)–S(1B)	110.6(3)
S(1A)–Sn(1A)–S(2A)	89.39(7)	S(1B)–Sn(1B)–S(2B)	90.01(8)
C(6A)–Sn(1A)–S(5A)^{i}	78.6(3)	C(6B)–Sn(1B)–S(5B)^{i}	79.3(4)
C(4A)–Sn(1A)–S(5A)^{i}	83.8(3)	C(4B)–Sn(1B)–S(5B)^{i}	81.8(3)
S(2A)–Sn(1A)–S(5A)^{i}	65.70(6)	S(2B)–Sn(1B)–S(5B)^{i}	65.38(6)
S(1A)–Sn(1A)–S(5A)^{i}	154.43(6)	S(1B)–Sn(1B)–S(5B)^{i}	155.29(7)
C(6A)–Sn(1A)–S(5A)^{ii}	85.0(3)	C(6B)–Sn(1B)–S(5B)^{iii}	83.5(5)
C(4A)–Sn(1A)–S(5A)^{ii}	80.2(3)	C(4B)–Sn(1B)–S(5B)^{iii}	78.7(3)
S(2A)–Sn(1A)–S(5A)^{ii}	150.40(6)	S(2B)–Sn(1B)–S(5B)^{iii}	151.31(6)
S(1A)–Sn(1A)–S(5A)^{ii}	61.69(6)	S(1B)–Sn(1B)–S(5B)^{iii}	61.56(7)
S(5A)^{i}–Sn(1A)–S(5A)^{ii}	143.68(6)	S(5B)^{i}–Sn(1B)–S(5B)^{iii}	143.15(6)
C(1A)–S(1A)–Sn(1A)	98.0(2)	C(1B)–S(1B)–Sn(1B)	97.3(3)
C(2A)–S(2A)–Sn(1A)	97.5(2)	C(2B)–S(2B)–Sn(1B)	97.5(3)
C(3A)–S(5A)–Sn(1A)^{iv}	109.4(3)	C(3B)–S(5B)–Sn(1B)^{iv}	109.4(3)
C(3A)–S(5A)–Sn(1A)^{v}	104.0(3)	C(3B)–S(5B)–Sn(1B)^{vi}	101.9(3)
Sn(1A)^{iv}–S(5A)–Sn(1A)^{v}	133.46(7)	Sn(1B)^{iv}–S(5B)–Sn(1B)^{vi}	124.17(6)
C(5A)–C(4A)–Sn(1A)	114.4(7)	C(5B)–C(4B)–Sn(1B)	116.7(8)
C(7A)–C(6A)–Sn(1A)	115.0(7)	C(7B)–C(6B)–Sn(1B)	121.3(11)

[a] Symmetry operations: (i) $x+1$, y, z; (ii) $x+1/2$, $-y$, $z-1/2$; (iii) $x+1/2$, $-y+1$, $z-1/2$; (iv) $x-1$, y, z; (v) $x-1/2$, $-y$, $z+1/2$; (vi) $x-1/2$, $-y+1$, $z+1/2$.

prior to the fusion point, but with only about a 27% weight loss by 400°C. To account for the lack of peaks in the cool/reheat cycles in the DSC experiments, both samples must have been completely changed on heating to 400°C without the formation of other fusible materials. The residues after the DSC experiments were dark-coloured amorphous materials.

Only the thin metallic-looking orange-coloured plates obtained from aqueous acetone were suitable for crystallography. Two independent molecules, A and B, are present in the asymmetric unit. The molecules, A and B, are similar with the differences basically arising from their orientation with respect to the unit cell edges. The atom numbering system used for each molecule is illustrated in Fig. 6a. Primary bonds to tin are formed by the two methyl groups and the chelating dmit dithiolato S atoms, S(1) and S(2). Molecules of each type are linked into chains via Sn–thione S intermolecular interactions in the direction of c: Sn(1)–S(5A)^{i} = 3.001(2) Å and Sn(2)–S(5B)^{ii} = 2.960(2) Å [symmetry operations: (i) x, $-y+1$, $z-1/2$; (ii) $-x+3/2$, y, $z+1/2$]. Each chain consists entirely of molecules of the one type. The five-coordinate tin centres have distorted trigonal bipyramidal arrays with the axial sites occupied by the intermolecular thione S and a thiolato S atom of a chelating dmit ligand: S(2A)–Sn(1)–S(5A)^{i} = 165.61(8) and S(2B)–Sn(1)–S(5B)^{i} = 167.57(8)°. The asymmetry in the chelate bonding to tin in **4** [Sn–S = 2.440(3) and 2.518(2) in molecule A, and 2.457(3) and 2.521(2) Å in molecular B] is similar to that in *ortho*-**3**. The Sn and thione S atoms are out of the best dmit plane by 0.273(4) and −0.133(5) Å, respectively, in molecule A, i.e. a chair-shaped [Sn(dmit)] fragment, while in molecule B, the values are −0.072(4) and −0.102(5) Å, respectively, i.e. a boat-shaped [Sn(dmit)] fragment. Also present are intra-chain S···S contacts [S(1A)···S(5A)^{i} and S(1A)···S(4A)^{i} = 3.486(3) and 3.537(3) Å; and S(1B)···S(5B)^{i} and S(1B)···S(4B)^{ii} = 3.502(3) and 3.564(3) Å], while further S···S contacts [S(4A)···S(4A)^{iii} = 3.379(4) in A, and S(4B)···S(4B)^{iv} = 3.561(4) and S(4B)···S(4B)^{v} = 3.355(4) Å in B] produce pair-wise association of the primary chains. There are separate and distinct chain pairs of type A and type B molecules: further S···S contacts [S(1A)···S(2B)^{vi} = 3.527(4) and S(5A)···S(3B)^{vii} = 3.561(3) Å link the chain pairs, of different type, to complete the connectivity, see Fig. 6b [symmetry operations: (i) x, $-y+1/2$, $z-1/2$; (ii) $-x+3/2$, y, $z-1/2$; (iii) $-x+1/2$, $-y+1/2$, z; (iv) $-x+3/2$, $-y+1/2$, z; (v) $-x+3/2$, $-y+1/2$, z; (vi) $-x+1/2$, y, $z-1/2$; (vii) $-x+1$, $-y+1$, $-z+1$] (Table 4).

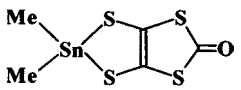

7

2.5. Comparison of structures of **2**–**4** and $Me_2Sn(dmio)$ (**7**)

Generally, a tin centre in an un-associated diorganotin dithiolate is coordinatively unsaturated and will coordinate, at least in the solid state, with available internal or external donor centres, unless other factors, such as steric hindrance, intervene [6]. This is illustrated by **3**, their 1,3-dithiole-2-one-4,5-dithiolato analogues, $R_2Sn(dmio)$, and diorganotin 1,2-ethanedithiolates, $R_2Sn(edt)$. Compounds, **2**–**4**, $(RO_2CCH_2CH_2)_2Sn(dmit)$, $(RO_2CCH_2CH_2)_2Sn(dmio)$ [7], $Me_2Sn(dmio)$ (**7**) [6], and [**II**: pyridine] [1,2] all confirm this. For solid $R_2Sn(edt)$, only thiolato S atoms are available for intermolecular coordination, with the formation of SSnSSn rings. The number and strength of the Sn–S interac-

tions depend on the R group, e.g. the intermolecular Sn–S bond length in penta-coordinate $Me_2Sn(edt)$ is 3.18 Å [8], in hexa-coordinate $Bu_2Sn(edt)$ 3.69 Å [9]: the compound, $^tBu_2Sn(dmit)$, remains un-associated [10]: there is a single long intermolecular Sn···S separation, 3.885 Å, in $Ph_2Sn(edt)$ [11], which is just within the sum of the van der Waals radii sum for Sn and S of 4.05 Å.

In the case of **7**, inter-molecular associations involve both a carbonyl O and a thiolato S atom and the production of six-coordinate tin, and again a SSnSSn ring is formed [6], which together give rise to an honeycomb arrangement, see Fig. 7a. This arrangement was not mentioned in our earlier paper [6].

The situation found for **II** is quite subtle as shown particularly with dimorphic **3**. However, it is clear that the additional, secondary and weaker interactions in **II** have only a small impact on the molecular geometry. Indeed, Mössbauer spectra of samples of **3** were similar ($\delta = 1.56 \pm 0.01$ mm s^{-1} and $\Delta = 2.78 \pm 0.03$ mm s^{-1}) irrespective of the crystallisation media. The same was found for **4** ($\delta = 1.40 \pm 0.01$ mm s^{-1} and $\Delta = 2.70 \pm 0.03$ mm s^{-1}): all peak widths at half heights in both cases were less than 1 mm s^{-1}. Mössbauer spectroscopy is clearly insufficiently sensitive to detect the small structural changes found for **3**.

The distortions from ideal trigonal bipyramidal arrays in **2**, *ortho*-**3**, and **4** are not the result of the presence of the chelate, since the chelate bite angles are near 90° in all cases. The distortion can be seen in the angles, in particular the axial $\angle$X–Sn–Y and the $\Sigma(\angle X_{ax}–Sn–Y_{eq})$ values for the two 'pyramidal' halves of each structure. The smallest angle at tin in each of **2**, *ortho*-**3**, and **4** (molecule B) involves the axial intermolecular thione–S and the equatorial thiolato–S, the values being 71.73(3), 70.74(10) and 79.98(8)°, respectively. The equivalent angle in **4** (molecule B) is

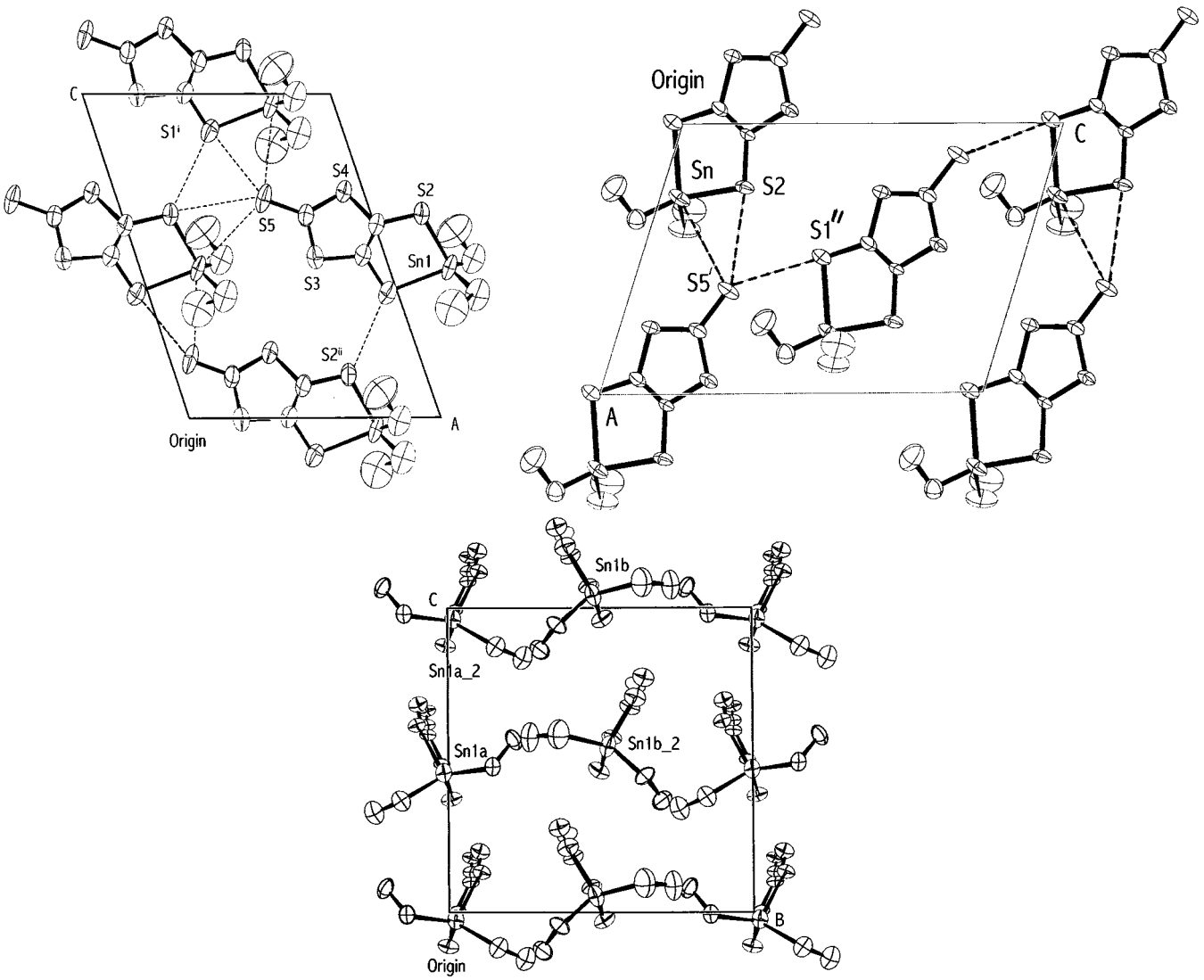

Fig. 5. Intermolecular interactions exhibited by molecules A (a) and molecules B (b) of *mono*-**3**. (c) The unit cell content of *mono*-**3** viewed down *a*, showing the layered structure; probability ellipsoids drawn at the 50% level.

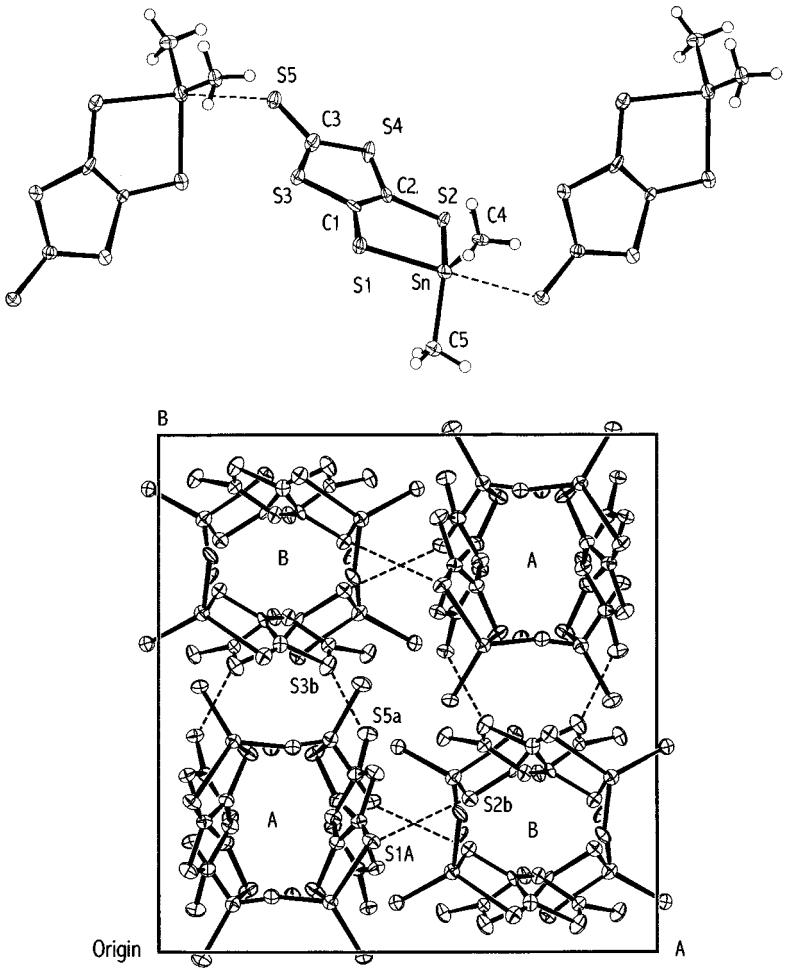

Fig. 6. (a) Part of a chain of molecules A of **4** linked by intermolecular Sn–thione S bonds, situation for molecules B is similar: common numbering systems are used; (b) interaction between chain-pairs of **4**; probability ellipsoids are drawn at the 50% level.

78.96(7), more or less the same as a C_{equat}–Sn–S–thione angle of 76.3(2)°. In general, the direction of approach of the intermolecular thione group to the tin centre appears to be the major cause of the distortion from a regular trigonal bipyamidal array. Similar distortions also arise in the trigonal bipyramidal anions of [Q][R_2SnX(dmit)] [2] and [Q][R_2SnX(dmio)] [6], where X is in an axial site (Cl, Br, I or SCN). The smallest angles at tin in these compounds are the X–Sn–S_{equat} angles, all ca 80°, with the X–Sn–S_{axial} angles being less than 170°. In contrast to the situation in **3**, **4** and **7**, there are no intermolecular S···S contacts less than the van der Waals radii sum in **2** between chains [6].

The geometry in the six-coordinate species, *mono*-**3** and **7** [6], are also far from regular: even severely distorted octahedral descriptions appear inappropriate. The dmio compound, **7**, forms a honeycomb network due to a combination of S···O, S···S and Sn–S and Sn–O intermolecular interactions: the rings are formed from six molecules, however, the arrangement is quite distinct from that found for *ortho*-**3**, see Fig. 7a. Of interest, the dmio ligands in **4** are stacked on top of each other in the direction of *b*, such that the ligands are virtually superimposed on one another, see Fig. 7b. The distance between the ring centroids is 3.847 Å, an ideal distance for π–π interactions. A comparison of selected geometric parameters for **2**–**4** and **7** and R_2Sn(edt) is presented in Table 5.

3. Experimental

Melting points were determined using a Kofler hot-stage. Solution NMR spectra were obtained on Bruker 250 MHz and Varian 400 MHz instruments. Solid state NMR spectra were recorded by the EPSRC service, based at the University of Durham. IR spectra were obtained on Philips Analytical PU 9800 FTIR and Nicolet 205 FTIR instruments. Powder diffraction was carried out on a Stoe STADI instrument, DSC and TGA studies on Mettler Toledo DSC 821^e and Meller Toledo TGA/SDTA 851^e coupled to Balzers Thermostar MS instruments. Mössbauer spectra were obtained by Professor Lorenzo Pellerito of the University

Table 4
Selected bond lengths (Å) and angles (°) in **4** at 150 K[a]

Molecule A		Molecule B	
Sn(1)–C(5A)	2.110(9)	Sn(2)–C(5B)	2.119(8)
Sn(1)–C(4A)	2.121(9)	Sn(2)–C(4B)	2.129(8)
Sn(1)–S(1A)	2.440(3)	Sn(2)–S(1B)	2.457(3)
Sn(1)–S(2A)	2.518(2)	Sn(2)–S(2B)	2.521(2)
Sn(1)–S(5A)^{i}	3.001(2)	Sn(2)–S(5B)^{iii}	2.960(2)
S(1A)–C(1A)	1.762(8)	S(1B)–C(1B)	1.759(8)
S(2A)–C(2A)	1.731(9)	S(2B)–C(2B)	1.758(9)
S(3A)–C(3A)	1.717(8)	S(3B)–C(3B)	1.699(8)
S(3A)–C(1A)	1.719(10)	S(3B)–C(1B)	1.735(9)
S(4A)–C(3A)	1.722(9)	S(4B)–C(3B)	1.731(9)
S(4A)–C(2A)	1.747(8)	S(4B)–C(2B)	1.723(8)
S(5A)–C(3A)	1.655(10)	S(5B)–C(3B)	1.671(9)
C(1A)–C(2A)	1.388(11)	C(1B)–C(2B)	1.356(11)
C(5A)–Sn(1)–C(4A)	124.9(4)	C(5B)–Sn(2)–C(4B)	126.0(4)
C(5A)–Sn(1)–S(1A)	112.9(3)	C(5B)–Sn(2)–S(1B)	115.3(3)
C(4A)–Sn(1)–S(1A)	116.4(3)	C(4B)–Sn(2)–S(1B)	115.4(3)
C(5A)–Sn(1)–S(2A)	101.3(2)	C(5B)–Sn(2)–S(2B)	98.8(2)
C(4A)–Sn(1)–S(2A)	102.5(2)	C(4B)–Sn(2)–S(2B)	99.4(2)
S(1A)–Sn(1)–S(2A)	89.03(8)	S(1B)–Sn(2)–S(2B)	89.04(8)
C(5A)–Sn(1)–S(5A)^{i}	90.7(2)	C(5B)–Sn(2)–S(5B)^{iii}	91.2(2)
C(4A)–Sn(1)–S(5A)^{i}	76.3(2)	C(4B)–Sn(2)–S(5B)^{iii}	80.4(2)
S(1A)–Sn(1)–S(5A)^{i}	78.96(7)	S(1B)–Sn(2)–S(5B)^{iii}	79.98(8)
S(2A)–Sn(1)–S(5A)^{i}	165.61(8)	S(2B)–Sn(2)–S(5B)^{iii}	167.57(8)
C(1A)–S(1A)–Sn(1)	99.6(3)	C(1B)–S(1B)–Sn(2)	98.7(3)
C(2A)–S(2A)–Sn(1)	96.8(3)	C(2B)–S(2B)–Sn(2)	97.4(3)
C(3A)–S(5A)–Sn(1)^{ii}	116.4(3)	C(3B)–S(5B)–Sn(2)^{iv}	114.1(3)

[a] Symmetry operations: (i) x, $-y+1/2$, $z-1/2$; (ii) x, $-y+1/2$, $z+1/2$; (iii) $-x+3/2$; y, $z-1/2$; (iv) $-x+3/2$, y, $z+1/2$.

of Palermo, Italy. Compounds, Me_2SnCl_2 and Bu_2SnCl_2 were commercial samples and used as such: R_2SnBr_2 (R = Et or n-$C_{14}H_{29}$) were obtained from reactions of Ph_2SnR_2 with Br_2 (1:2 mole ratio) in $CHCl_3$ at 25°C.

3.1. Synthesis

Compounds **3–5** were obtained by a simplified adaptation of a previously reported procedure, from $[NEt_4]_2[Zn(dmit)_2]$ and R_2SnX_2 (X = Cl or Br) in Me_2CO [2]. The solution of the reagents (1:1 mole ratio: 2–4 mmol) in acetone (40–80 ml) was agitated in an ultrasonic bath for 10–30 min, an equal volume of water added, and the solid collected after standing for 30 min. Further recrystallisations were carried out in particular solvents. All products had solution ^{1}H-, ^{13}C- and ^{119}Sn-NMR spectra in Me_2CO-d_6 solution in agreement with that published [2]. Compound, (n-$C_{14}H_{29})_2$Sn(dmit), **6**, a new compound, was obtained by a similar procedure.

3.1.1. Compound *3*

A first batch of crystals was obtained as deep-orange needles by the direct addition of water to the reaction mixture. Anal. Found: C, 22.9; H, 2.7. Calc. for

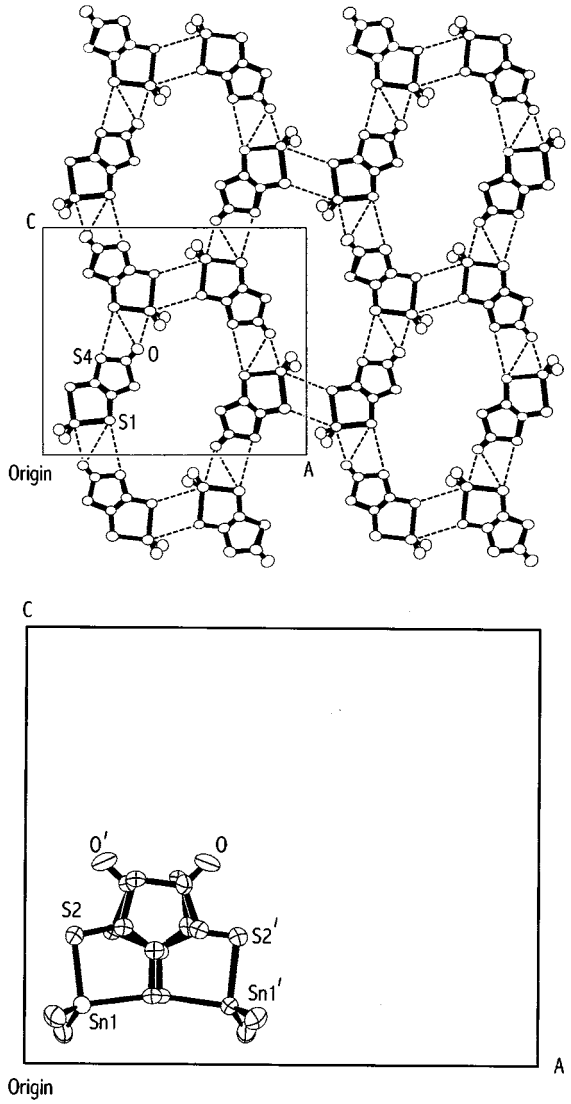

Fig. 7. (a) The honeycomb network of molecules of **7**, arising from Sn–S, Sn–O, S···S and S···O interactions; (b) stacking of dmio units, in the direction of b, of **7**, probability ellipsoids are drawn at the 50% level.

$C_7H_{10}S_5Sn$: C, 22.5; H, 2.7%. IR (CsI, cm^{-1}):ν 1445, 1178, 1022, 894, 677, 527, 516, 489, 460, 349, 268. ^{13}C-NMR (Me_2CO-d_6, 62.9 MHz): δ 10.4 (J [^{119,117}Sn–^{13}C] = 41.1 Hz, Me), 20.4 (J [^{119,117}Sn–^{13}C] = 492, 470 Hz, CH_2), 130.4 (C=C), 211.2 (C=S). ^{119}Sn-NMR (Me_2CO-d_6; 93.3 MHz): δ 164.8 (lit. value [2] = 165.7). ^{13}C-NMR (solid state, 75.4 MHz, relaxation delay 1.0 s, cross-polarisation with flip-back): δ 11.6, 12.5, 13.1, 13.5 (Me), 21–28 (envelope with spikes at 22.1, 23.5,2 4.7, 25.2 and 26.6) (CH_2), 132.8, 133.9, 134.3, 135.3 and 136.8 (C=C), 205.3, 206.3 (C=S). ^{119}Sn-NMR (solid state, 111.9 MHz, relaxation delay 1.0 s, cross-polarisation with flip-back): δ 112.1, 123.4, 158.2.

A further recrystallisation was achieved on slow evaporation of an acetone solution. The crystals were red in colour. This batch was subsequently shown to be

the orthorhombic form of **3**, *ortho*-**3**. IR (CsI, cm^{-1}):*v* 1438, 1180, 1019, 894, 680, 531, 516, 489, 462, 334, 272. Anal. Found: C, 23.0; H, 2.6. Calc. for $C_7H_{10}S_5Sn$: C, 22.5; H, 2.7%. Recrystallisation from aqueous MeOH gave the monoclinic form, *mono*-**3**, as red needles. IR: same as the orthorhombic form.

3.1.2. Compound **4**

A first batch of deep-orange crystals was obtained by direct addition of water to the reaction mixture. IR (CsI, cm^{-1}): *v* 1439, 1036, 1028, 926, 892, 787, 765, 551, 534, 516, 460, 440, 360, 336, 274. Anal. Found: C, 17.9; H, 1.7. Calc. for $C_5H_6S_5Sn$: C, 17.4; H, 1.8%. ^{13}C-NMR (Me_2CO-d_6, 62.9 MHz):δ 9.3 (J [^{119,117}Sn–^{13}C] = 517, 495 Hz, Me), 130.0 (C=C), 210.9 (C=S). ^{119}Sn-NMR (Me_2CO-d_6, 93.3 MHz):δ 143.6. A second recrystallisation was achieved from aqueous MeOH. Anal. Found: C, 17.0; H, 2.0. Calc. for $C_5H_6S_5Sn$: C, 17.4; H, 1.8%. IR: as above.

3.1.3. Compound **5**

Addition of water to the reaction mixture produced an orange-coloured powder, which was successively recrystallised from acetone–petroleum ether (40:60) and MeOH. The two crystalline samples had the same spectral properties and similar analytical findings. Anal. Found: C, 31.0; H, 4.2. Calc. for $C_{11}H_{18}S_5Sn$: C, 30.8; H, 4.2 (recryst. acetone–petroleum ether); C, 30.9; H, 4.1% (recryst. MeOH). IR (KBr, cm^{-1}):*v* 1438, 1012. ^{13}C-NMR (Me_2CO-d_6, 62.9 MHz) δ 13.8 (Me), 26.7 (J [^{119,117}Sn–^{13}C] = 94, 90 Hz, Me$\underline{C}H_2$), 27.5 (J [^{119,117}Sn–^{13}C] = 455, 434 Hz, CH_2Sn), 28.5 (J [^{119,117}Sn–^{13}C] = 36 Hz, $\underline{C}H_2CH_2Sn$), 130.3 (C=C), 211.3 (C=S). ^{119}Sn-NMR (Me_2CO-d_6, 93.3 MHz): δ 157.5; lit. value [2] 161.5.

3.1.4. Compound **6**

Addition of water to the reaction mixture, containing (n-$C_{14}H_{29}$)$_2$$SnCl_2$ and $[NEt_4]_2[Zn(dmit)_2]$, produced an orange-coloured powder, which was recrystallised from acetone–petroleum ether (40:60), m.p 179–174°C. Anal. Found: C, 53.0; H, 8.4. Calc. for $C_{31}H_{58}S_5Sn$: C, 52.5; H, 8.2%. IR (KBr, cm^{-1}):*v* 1471, 1441, 1063, 1026. ^{13}C-NMR (Me_2CO-d_6, 62.9 MHz): δ 14-3–33.7 (alkyl), 130.3 (C=C), 211.5 (C=S). ^{119}Sn-NMR (Me_2CO-d_6, 93.3 MHz]: δ 163.1.

Table 5
Comparison of selected geometric parameters for **2**–**4** and **7** and $R_2Sn(edt)$

Compound	Primary Sn–S bonds (Å)	Secondary bonds to tin (Å)	C–Sn–C (°)	S···S	References
$Me_2Sn(dmit)$ (**4**)					This study
Mol A	2.440(3) and 2.518(2)	3.001(2): to thione S	124.9(4)	3.486(3), 3.537(3), 3.3799(4)	
Mol B	2.457(3) and 2.521(2)	2.960(2): to thione S	126.0(4)	3.564(3), 3.502(3), 3.355(4), 3.561(4), 3.527(4)	
PhMeSn(dmit) (**2**)	2.437(1) and 2.487(1)	3.139(1): to thione S	115.8(1)	3.315(2)	[2]
				3.446(2)	
$Et_2Sn(dmit)$ (**3**)					This study
ortho at 150 K	2.4590(14)	3.0083(15)	130.8(2)	3.1721(18), 3.5372(19), 3.509(2), 3.4695(19)	
ortho at 298 K	2.5235(15)	3.037(4)	128.7(8)		
mono (A)	2.436(4) and 2.513(4)	3.567(2) and 3.620(3)	126.3(3)	3.272(3), 3.396(6), 3.511(4)	
mono (B)	2.449(2) and 2.460(2) 2.447(3) and 2.458(3)	3.555(2) and [3.927(2)]-all to thione S	119.5(5)	3.374(3), 3.503(4)	
$Me_2Sn(edt)$	2.412(1) and 2.472(1)	3.180(1)	121.4(2)		[8]
$Bu_2Sn(edt)$	2.414(2)	3.688(3)	122.6		[9]
$^tBu_2Sn(edt)$	2.411(3) and 2.417(3)	–	118.5(3)		[10]
$Ph_2Sn(edt)$	2.408(5) and 2.424(5)	3.885	116.4(6)		[11]
$Me_2Sn(dmio)$ (**7**)	2.440(2) and 2.687(2)	2.648(4): to one O	124.2(4)	3.258(4) (O···S)	[6]
		3.645(3): to thiolato S		3.598(3)	

Table 6
Crystal and refinement data

	mono-**3**	*ortho*-**3**	*ortho*-**3**	**4**
Empirical formula	$C_7H_{10}S_5Sn$	$C_7H_{10}S_5Sn$	$C_7H_{10}S_5Sn$	$C_5H_6S_5Sn$
Formula weight	373.14	373.14	373.14	345.09
T (K)	298(2)	150(2)	298(2)	150(2)
Wavelength (Å)	0.71073	0.71073	0.71073	0.71073
Crystal system	Monoclinic	Orthorhombic	Orthorhombic	Orthorhombic
Space group	*Pn*	*Pna*2(1)	*Pna*2(1)	*Pccn*
Unit cell dimensions				
a (Å)	9.1408(3)	10.8927(7)	11.149(7)	16.3382(13)
b (Å)	11.7714(4)	12.8560(8)	12.843(6)	17.1930(15)
c (Å)	12.6359(3)	8.9562(5)	8.991(8)	14.7079(9)
α (°)	90	90	90	90
β (°)	107.5077(18)	90	90	90
γ (°)	90	90	90	90
Volume (Å^3)	1296.64(7)	1254.20(13)	1287.4(15)	4131.5(5)
Z	4	4	4	16
Calculated density (Mg m^{-3})	1.911	1.976	1.9125	2.219
Absorption coefficient (mm^{-1})	2.732	2.852	2.752	3.420
F(000)	728	728	728	2656
Crystal colour	Deep red	Deep red	Deep red	Metallic golden brown
Crystal size (mm)	$0.40\times0.30\times0.20$	$0.30\times0.20\times0.20$	$0.46\times0.20\times0.16$	$0.10\times0.10\times0.01$
θ Range for data collection (°)	1.73–26.36	2.45–26.37	2.42–25.04	1.72–26.34
Index range	$-11\le h\le11$ $-14\le k\le14$ $-15\le l\le15$	$-13\le h\le13$ $-14\le k\le15$ $-10\le l\le11$	$0\le h\le13$ $0\le k\le15$ $0\le l\le10$	$-20\le h\le20$ $-15\le k\le21$ $-18\le l\le18$
Reflections collected/unique	20 230/5285 ($R_{Int}=0.0514$)	6563/2303 ($R_{Int}=0.0415$)	1222/1221 ($R_{int}=0.0044$)	21 441/4215 ($R_{int}=0.2007$)
Completeness to 2θ	99.6%	99.9%	100%	100%
Absorption correction	Multi-scan	Multi-scan	None	Multi-scan
Max. and min. transmission	0.783 and 0.635	0.759 and 0.684	0.6672 and 0.3642	0.998 and 0.955
Refinement method	Full-matrix least-squares on F^2	Full-matrix least-squares on F^2	Full-matrix least-squares on F^2	Full-matrix least-squares on F^2
Data/restraints/parameters	5285/2/239	2023/1/121	1221/1/120	4215/0/203
Goodness-of-fit on F^2	1.023	1.048	0.983	0.907
Final R indices [$I>2\sigma(I)$]	$R_1=0.0423$ $wR_2=0.0962$	$R_1=0.0315$ $wR_2=0.0720$	$R_1=0.0419$ $wR_2=0.0758$	$R_1=0.0512$ $wR_2=0.0735$
R indices (all data)	R1 = 0.0612 $wR_2=0.1051$	$R_1=0.0351$ $wR_2=0.0739$	$R_1=0.0660$ $wR_2=0.0798$	$R_1=0.0512$ $wR_2=0.0735$
Flack x parameter [a]	−0.03(3)	0.40(3)	0.02(6)	
Largest difference peak and hole (e Å^{-3})	1.032 and −1.086	1.162 and −1.439	0.733 and −0.456	0.937 and −1.007

[a] Absolute structure parameter.

3.2. Crystallography

The intensity data for *ortho*-**3**, recrystallised from acetone, collected at 298 K, were obtained using a Nicolet P3 4-circle diffractometer with θ–2θ scan modes and 2θ maxima as 50°. Cell refinement and data collection: Nicolet P3 software; data reduction: RDNIC [12]. Correction for absorption based on Ψ-scans was unsuccessful as it resulted in unrealistic (non-positive definite) thermal vibration parameters for certain atoms which had refined satisfactory with the uncorrected data; in any case the Ψ-cans showed little variation in the intensity.

The intensity data for *ortho*-**3** and **4**, both collected at 150 K, and *mono*-**3**, collected at 298 K, were obtained with the Enraf Nonius Kappa CCD diffractometer of the EPSRC's National data collection center at the University of Southampton. Cell refinement and data collection and reduction: DENZO [13] and COLLECT [14]: correction for absorption: SORTAV [15]. All structures were solved (SHELXS-86) [16] by standard heavy atom methods, although *mono*-**3** proved to be rather more demanding than the others. In this case, the initial solution of the structure in the space group $P2_1/n$ yielded an image corresponding to the two molecules of the asymmetric unit superimposed with Sn in common. That portion of the image corresponding to molecule A was isolated unchanged while that of molecule B was translated by the operation of a crystallographic centre of symmetry along with a copy of the tin atom. The y

coordinates of all atoms were then adjusted for compatibility with the standard setting of the space group *Pn* with the origin on the *n*-glide plane and the refinement completed in this space group. Certain of the C–C bond lengths within the ethyl groups of the *ortho*-**3** (C5–C6) and *mono*-**3** (C5B–C6B and C7B–C8B) at ambient temperature appear unrealistically short. The program, SHELXL-97 [17], suggested that C6B may be split but in the absence of any structural justification for doing so, this option was investigated but not pursued. This, together with the large amplitude of thermal vibration associated with these atoms, shows that they are subject to disorder and are as a consequence comparatively poorly defined. For all of the structures SHELXL-97 was used for refinement and the preparation of the published and deposited data. Of the polar (non-centrosymmetric) structures of **3**, absolute structures were obtained for *mono*-**3** and *ortho*-**3** at 298 K. For *ortho*-**3** at 150 K the sample crystal was found to have been twinned necessitating the use of the SHELXL-97 TWIN and BASF instruction pair and hence rendering the absolute structure indeterminate. Crystal and refinement data for the compounds are listed in Table 6

4. Supplementary data

Crystallographic data for the structural analysis have been deposited with the Cambridge Crystallographic Data Centre, CCDC Nos. 154944–154947 for *mono*-**3** at 298 K, *ortho*-**3** at 150 K, *ortho*-**3** at 298 K and **4** at 150 K, respectively. Copies of this information may be obtained free of charge from The Director, 12 Union Road, Cambridge CB2 1EZ, UK (fax: +44-1223-336033; e-mail: deposit@ccdc.cam.ac.uk of www: http:www.ccdc.cam.ac.uk).

Acknowledgements

The authors thank the ESPSRC X-ray service at the University of Southampton for the low temperature data, and Professor L. Pellerito, Palermo, for the Mössbauer spectra.

References

[1] (a) S.M.S.V. Doidge-Harrison, R.A. Howie, J.T.S. Irvine, G.M. Spencer, J.L. Wardell, J. Organomet. Chem. 414 (1991) C5. (b) J.H. Aupers, Z.H. Chohan, P.J. Cox, S.M.S.V. Doidge-Harrison, R.A. Howie, A. Khan, G.M. Spencer, J.L. Wardell, Polyhedron 17 (1998) 4475.
[2] S.M.S.V. Doidge-Harrison, J.T.S. Irvine, A. Khan, G.M. Spencer, J.L. Wardell, J.H. Aupers, J. Organomet Chem. 516 (1996) 199.
[3] (a) E. Cerrada, S. Elipe, M. Laguna, F. Lahoz, A. Moreno, Synth. Met. 102 (1999) 1759. (b) E. Cerrada, E.J. Fernez, M.C. Gimeno, A. Laguna, M. Laguna, R. Terroba, M.D. Villacampa, J. Organomet. Chem. 492 (1995) 105.
[4] A.L. Spek, PLATON, University of Utrecht, The Netherlands, 2000.
[5] J.E. Huheey, E.A Keiter, R.L. Keiter, Inorganic Chemistry, Principles of Structure and Reactivity, 4th ed., Harper Collins, New York, 1993.
[6] Z.H. Chohan, R.A. Howie, J.L. Wardell, J. Organomet. Chem. 577 (1999) 140 (and references therein).
[7] (a) R. Balasubramanian, Z.H. Chohan, S.M.S.V. Doidge-Harrison, R.A. Howie, J.L. Wardell, Polyhedron 16 (1997) 4283. (b) H. Buchanan, R.A. Howie, A. Khan, G.M. Spencer, J.L. Wardell, J.H. Aupers, J. Chem. Soc. Dalton Trans. (1996) 541.
[8] (a) M. Drager, Z. Anorg. Allg. Chem. 477 (1981) 154. (b) A.S. Secco, J. Trotter, Acta Crystallogr. C 39 (1983) 451.
[9] A.G. Davies, S.D. Slater, D.C. Povey, G.W. Smith, J. Organomet. Chem. 352 (1988) 283.
[10] P.A. Bates, M.B. Hursthouse, A.G. Davies, S.D. Slater, J. Organomet. Chem. 363 (1989) 45.
[11] A.P.G. de Sousa, R.M. Silva, A. Cesar, J.L. Wardell, J.C. Huffman, A. Abras, J. Organomet. Chem. 605 (2000) 82.
[12] R.A. Howie, RDNIC, Data Reduction Program for Nicolet P3/R3 Diffractometer, University of Aberdeen, Scotland, 1980.
[13] Z. Otwinowski, W. Minor, in: C.W. Cater, R.M. Sweet (Eds.), Methods in Enzymology. In: Macromolecular Crystallography, Part A, vol. 276, Academic Press, New York, 1997, pp. 307–326.
[14] R. Hooft, COLLECT, Nonius BV, Delft, The Netherlands, 1998.
[15] (a) R.H. Blessing, Acta Crystallogr. A 51 (1995) 33. (b) J. Appl. Crystallogr. 30 (1997) 421.
[16] G.M. Sheldrick, Acta Crystallogr. A 46 (1990) 476.
[17] G.M. Sheldrick, SHELXL-97, Program for Crystal Structure Refinement, University of Göttingen, Germany, 1997.